24th EUROPEAN ROTORCRAFT FORUM

Marseilles, France - 15th-17th September 1998

AE 09

Numerical Study of the Unsteady Flow on a Pitching Airfoil with Oscillating Flap

by

W.Geissler, H.Sobieczky, H.Vollmers

DLR Institute of Fluid Mechanics, Bunsenstr.10, 37073 Göttingen, Germany

In recent years it has been demonstrated that with Higher Harmonic Control (HHC) technology the Blade-Vortex Interaction noise (BVI) level of a helicopter rotor in descent flight condition could be reduced by as much as 6dBA. Utilizing Individual Blade Control (IBC) systems even more benefit could be achieved. In the present joint program RACT (Rotor Active Control Technology) between Eurocopter Deutschland (ECD), Deutsches Zentrum für Luft- und Raumfahrt (DLR) and Daimler-Benz Research Institute (DB), an important further step is envisaged: Each blade is to be controlled individually by a moving trailing edge flap located at a limited radial section with high aerodynamic efficiency.

Before applying this complex technology to a full size rotor a windtunnel model has been developed representing a two-dimensional section of the blade with an active trailing edge flap. A system of piezoelectric actuators is installed inside the model to operate the flap. In addition to the flap motion the complete wind tunnel model is allowed to oscillate in pitching mode to simulate cyclic pitch of the rotor blade.

Overall forces and moments, pressure and flow field data have been measured instantaneously during tests in the Transonic Windtunnel Göttingen (TWG) of DLR.

In addition to the experiments numerical calculations have been carried out at DLR to

1) Provide steady and unsteady force and moment data for design of the actuator system, windtunnel model and model suspension rig,

2) Recalculate experimentally measured parameter variations for code validation purposes,

3) Gain insight into the complex physics of the flow and obtain new guidelines for the improvement of the codes.

1. Introduction

After the successfull application of Higher Harmonic Control (HHC) and Individual Blade Control (IBC) concepts the consequent further step is to influence a rotor blade individually at a position of high aerodynamic efficiency.

This Local Blade Control (LBC) concept can be utilized in different ways: either by deforming the leading edge of the blade if dynamic stall is to be influenced favorably [1], or by deforming the blade trailing edge as a measure to reduce locally steady and/or unsteady airloads for either noise reduction or vibration minimization. A moving trailing edge flap is a reasonable means to reduce both high speed impulsive noise (HSI) and blade vortex interaction noise (BVI) levels. This has recently been demonstrated by different groups of researchers i.e. [2], [3].

In Germany the concept to equip the blade with a moving trailing edge flap has been envisaged in the joint project RACT (Rotor Active Control Technology) between Eurocopter Deutschland (ECD), Daimler-Benz Research Institute (DB) and Deutsches Zentrum für Luft- und Raumfahrt (DLR) [4].

A windtunnel model has been developed including a trailing edge flap system driven by a set of piezoelectric actuators integrated inside the windtunnel model. The model itself is installed in the dynamic test rig of the DLR Institute of Aeroelastic in Göttingen.

A system of numerical codes has recently been developed in DLR to calculate the flow on oscillating airfoils including dynamic airfoil deformation [1]. In the present investigations these numerical tools will be applied to a typical helicopter airfoil section oscillating in pitching mode with additional oscillations of the trailing edge flap up to the 5th harmonics of the basic frequency of the blade (7Hz).

It will be shown that good correspondence between numerical and experimental data has been achieved. The effectiveness of the code for getting detailed insight into the complicated steady and unsteady flows involved will be demonstrated.

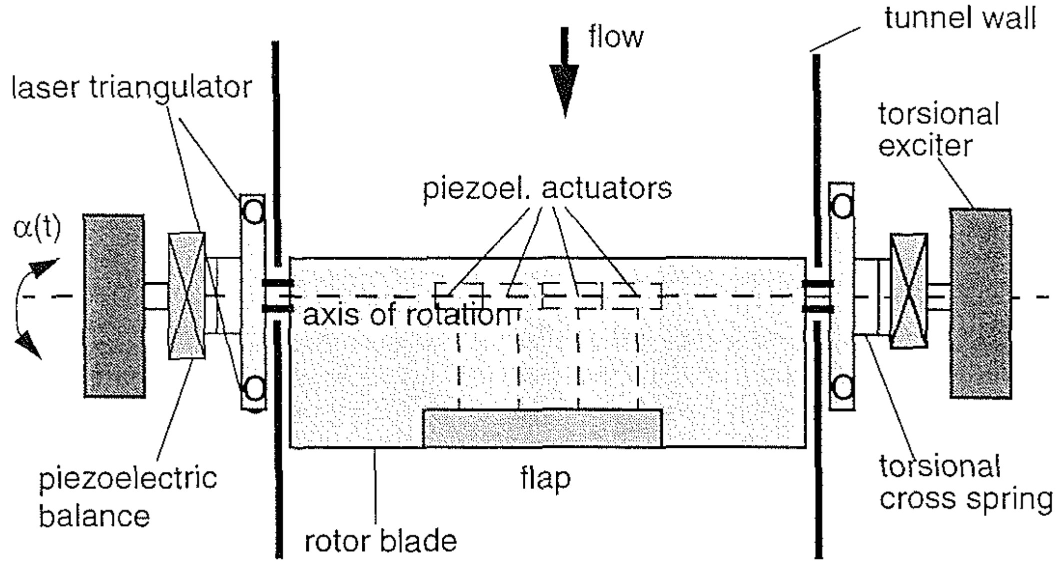

Fig. 1: Test Setup in the DLR Transonic Windtunnel Göttingen (TWG)

2. Wind Tunnel Test.

Fig.1 shows schematically the test setup in the 1mx1m test section of the DLR TWG windtunnel. The model of c=0.3m chord and 1m span is suspended in the dynamic test rig of DLR-Institute of Aeroelastic, [5]. The model is driven by hydraulic actuators on both sides of the rotation axis from outside the tunnel. The rotor blade section is equipped with an active trailing edge flap with 15% chord. The spanwise extension of the flap is 0.5m. The flap is deflected by a system of four piecoelectric actuators integrated inside the blade model. The aerodynamic measurements are obtained using

pressure sensors with a set of 49 in-situ pressure transducers (Kulites) distributed along the mid-section of the model,

a piezoelectric balance system arranged outside the model (see Fig.1) to measure steady and unsteady force- and moments of the complete model,

the DLR PIV measuring system of the DLR Institute of Fluid Mechanics for the measurement of the instantaneous flow field at selected model parameter settings [6].

Further details of the comprehensive tests are outlined in [5].

3. Numerical Code Development.

In recent years a concept has been proposed by DLR to dynamically deform the leading edge of a helicopter airfoil. Utilizing this "nose-droop" concept the dynamic stall phenomenon could favorably be influenced or even completely suppressed [1]. Numerical tools have been developed for this purpose and the efficiency of the device has successfully been demonstrated.

In the present study a dynamically moving trailing edge flap is used. The flap is sealed, i.e. the surface between the airfoil and the flap is smooth at each instant of time and no pressure compensation between upper and lower surface is possible, **Fig.2**.

Before numerical calculations on an airfoil with oscillating trailing edge flap can start, a set of airfoil shapes including the instantaneous flap positions have to be specified by means of the Geometry Generator System of DLR, [7].

This set of shapes represents the movement of the flap during a complete cycle of flap motion. Once the shapes have been specified the present grid generation procedure can be used to calculate complete grids about the instantaneous airfoil/flap geometries.

With this preparation the actual flow calculation can start. For the numerical flow calculation a 2D-time-accurate Navier-Stokes code is used which has successfully been applied to a variety of flow cases [8]. To apply the code for the present purpose of an airfoil

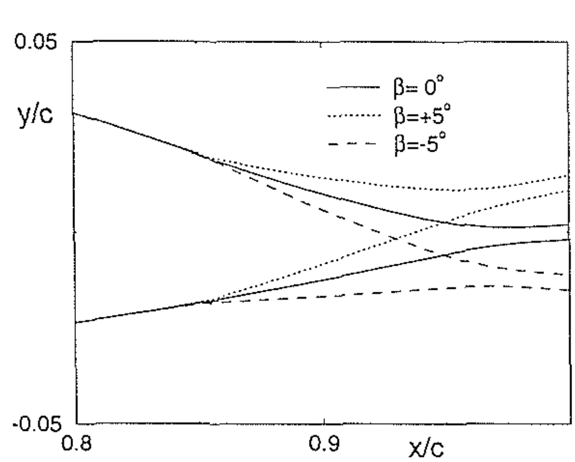

Fig. 2: Sealed Flap, Definition of Flap Deflection Angle

including a moving trailing edge flap several additional options had to be implemented:

- airfoil fixed, flap in periodic motion
- airfoil in pitching motion (1/ref), flap in additional motion with 2/ref...5/ref.
- both airfoil and flap in motion, variation of phase between airfoil and flap motion.

Since the windtunnel model is equipped with these additional options the numerical code should be able to simulate these cases as well.
In recent years specific concern was attributed to the problem of turbulence and transition modeling. In the present case of rather high Reynolds number flow it is assumed that the flow is fully turbulent. However it must be emphasized that this assumption is not valid in all cases (see [9]). Due to the fact that no information concerning transition behavior was available from the test the calculations were done with the fully turbulent assumption.
With the implementation of different turbulence models into the code a choice of more sophisticated models was possible. The Spalart-Allmaras one-equation model [10] was chosen for the present investigations. This model has proven to be superior to other models in cases of unsteady separation (dynamic stall) as well as in flow cases where strong shock waves occur. Location and strength of shock waves could be determined more accurately compared with results from the Baldwin-Lomax model.

Fig.3: Calculated and Measured Lift

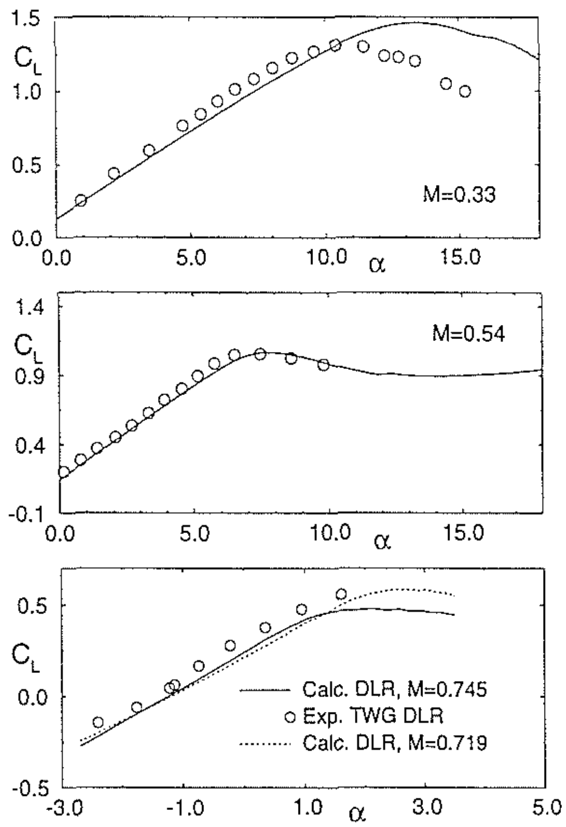

4. Results

The experiments in the TWG windtunnel were carried out at Mach numbers M=0.33, M=0.54 and M=0.74 respectively to cover retreating, neutral and advancing azimuthal blade positions.
During the tests the tunnel test section with the perforated walls was installed. This test section has an open aerea of the side walls of 6%. A corresponding wind tunnel wall correction,[11],[12] (see next section) was necessary to transfer to free flight conditions. The correction of steady airfoil incidences is straight forward. However in the present oscillating airfoil and/or flap cases a suitable correction procedure is not known from literature. In the present comparisons with numerical data only the **steady** mean incidence has been corrected. The amplitudes of oscillation remained unchanged.
In future tests in the TWG windtunnel it is recommended to use the available adaptive test section of the tunnel instead. In this test section the steady mean incidence can be corrected in an optimal way.
Fig.3 shows calculated and measured lift curves versus incidence for the three Mach numbers frequently investigated during the present tests. In the calculations the Spalart/Allmaras turbulence model was applied in all cases. The lift distributions show some deviations in the small Mach number case (M=0.33): the predicted maximum lift is not reached in the test. The reason is not completely understood but may be due to the rather large wind tunnel correction in the high incidence regime. In the higher Mach number cases the correspondence between calculation and experiment is satisfactory.
In the highest Mach number case M=0.745 a Mach number correction was applied in addition. The dotted curve in the lower Fig.3 shows improvements of C_{Lmax} compared to experiments.
The following parameter cases have been investigated:

- airfoil fixed, flap fixed (with/without steady flap deflection)
- airfoil oscillating (7Hz), flap in steady position
- airfoil fixed, flap oscillating (7Hz-35Hz), different flap deflection amplitudes
- airfoil oscillating (7Hz), flap oscillating (7Hz-35Hz)
- airfoil oscillating (7Hz), flap oscillating (7Hz-35Hz), 60°-steps of phase shift between airfoil and flap motion

From the large amount of data only some few results have been selected for the present paper. The following discussion of results is subdivided into three parts in reference to the three Mach numbers investigated.

4.1 Windtunnel correction.

The perforated test section was used for the wind tunnel experiments in the TWG. For this test section corrections in both incidence and Mach number are necessary. Following [11],[12] the incidence correction has to be:

$$\Delta\alpha = \lambda_o \cdot \delta_o$$

with

$$\delta_o = -0.250 \tag{1}$$

$$\lambda_o = (c \cdot C_L)/(2h)$$

c = chord of airfoil
2h = wind tunnel height
C_L =lift coefficient

Mach number correction:

$$M_c = M_\infty \cdot \left(1 + \left(1 + \frac{\kappa - 1}{2} \cdot M_\infty^2\right) \cdot \varepsilon_B\right) \tag{2}$$

with

$$\varepsilon_B = \frac{\pi \cdot A \cdot \Omega_s}{24 \cdot \beta^3 \cdot h^2}$$

and
Ω_S = -0.50
A = d . l (d=airfoil thickness: 0.012m, l = span: 1m)

$$\beta = \sqrt{1 - M_\infty^2}$$

as the Prandtl factor.

4.2 Machnumber M=0.33.

Figs.4a-c display forces, moments (4a), airfoil and flap deflections (4b) as well as pressure and skin friction distributions (4c) at selected azimuthal angles for a case of fixed airfoil and oscillating flap. Fig.4d shows details of the pressure distributions in the flap area. Legends in both Figs.4c and 4d are compatible. In Fig.4d the full symbols characterize the airfoil lower surface.
Comparisons of calculated and measured results are indicated in the graphs. The experimental force and moment data were integrated from 49 in situ pressure sensors (Kulites), indicated by "cp" in the graphs and directly measured by the piecoelectric

Fig.4: Airfoil Fixed, Flap in Motion

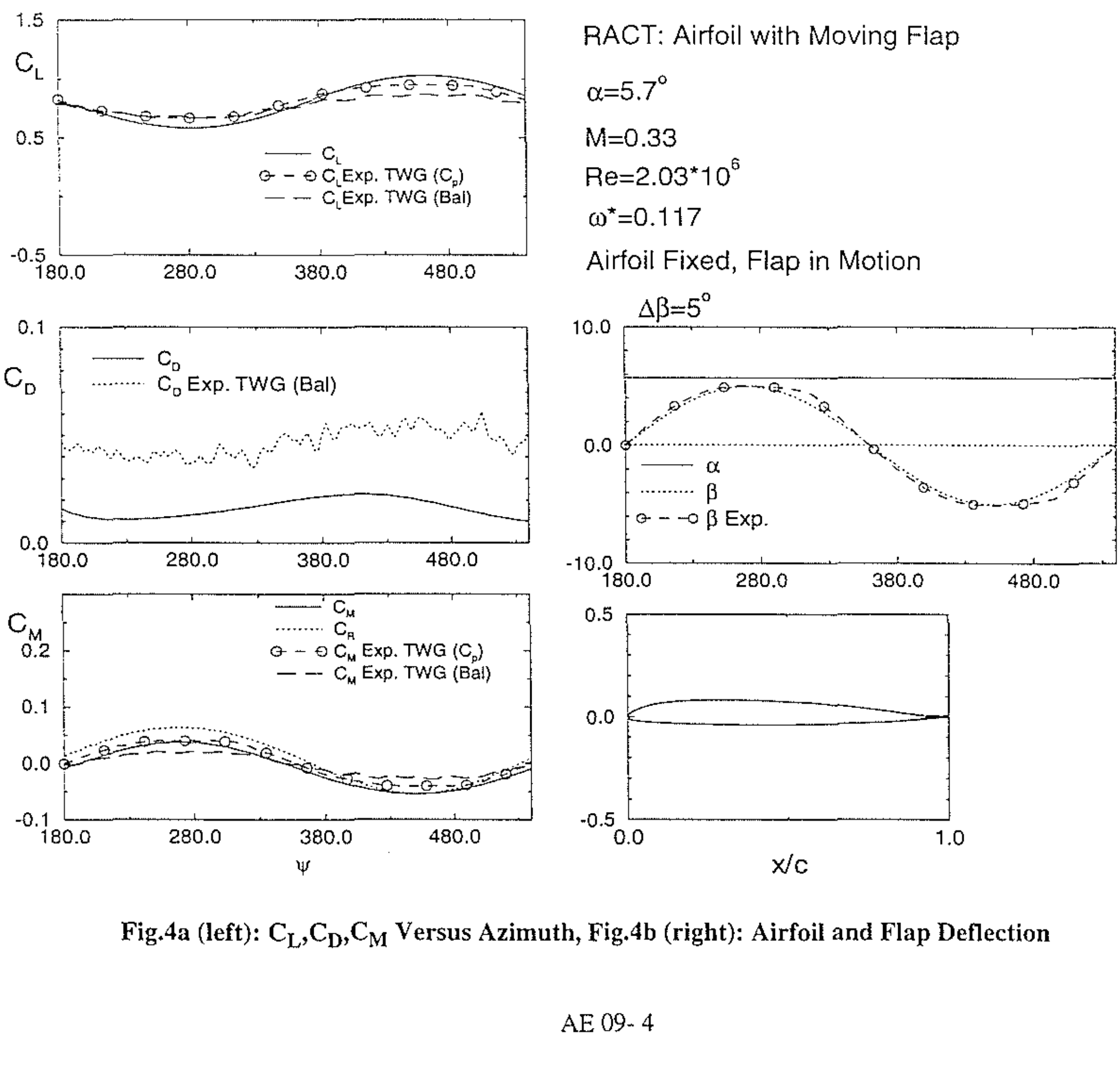

Fig.4a (left): C_L,C_D,C_M Versus Azimuth, Fig.4b (right): Airfoil and Flap Deflection

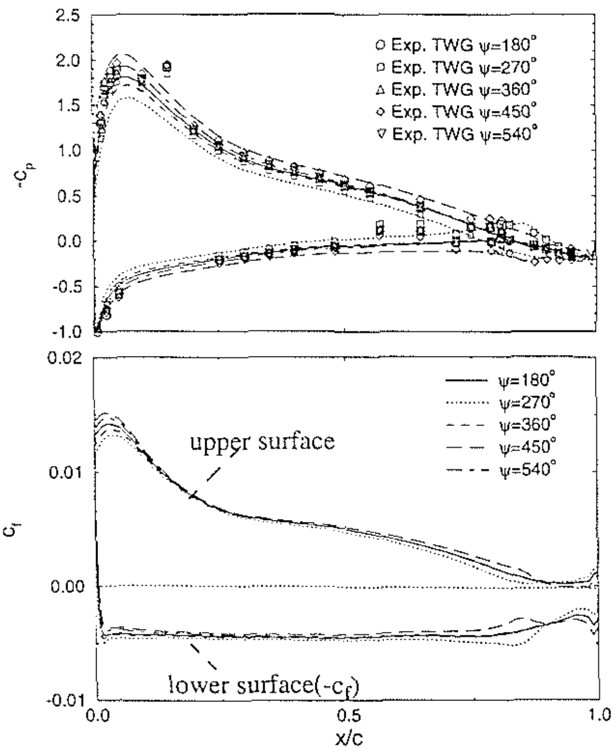

Fig.4c (left): Pressure- and Skinfriction at Selected Azimuth Angles.

Fig. 4d (down): Pressure Details in Flap Area

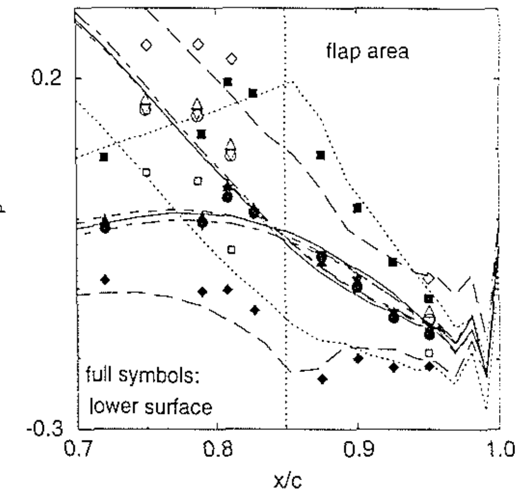

balances installed outside the windtunnel (see Fig.1) indicated by "Bal" in the corresponding graphs. The total drag coefficients could only be measured by the balances. A difference between integrated data from pressure sensors and results from the balances is to be expected due to the fact that the balances measure the aerodynamic forces of the **complete** model including effects from the windtunnel side walls and from the final spanwise extension and the side edges of the flap. These three dimensional effects are not considered in the numerical calculation which is strictly two dimensional.

The correspondence between calculation and experiment is very good except for the drag-coefficient in Fig.4a: the experimental data obtained from the piecoelectric balances show the well known offset in the steady mean value. The pressures in Fig.4c are in good agreement as well. This can be detected from Fig.4d showing the details in the flap area. The measured pressure coefficient at 15% chord upper surface seems to have a slightly wrong value as can be found also in following figures.

The slightly reduced C_{Lmax} and C_{Lmin} values of the test datas compared to calculation (Fig.4a,upper) can be attributed to a missing correction of the flap amplitude in the calculation. To apply a kind of "unsteady" correction to find the effective flap amplitude is not an easy task and has therefore not been tried. In future investigations the development of a corresponding correction procedure should be envisaged as well. If the adaptive wind tunnel test section is used the steady mean incidence and Mach number can be corrected in an optimal way. Only the additional amplitude effect has then to be corrected at least in a quasi steady manner.

Figs.5a-c show a case of the oscillating airfoil (1/ref, corresponding to 7Hz) with 2/ref (14Hz) oscillating flap.

Fig. 5a includes again lift-, drag- and pitching moment distributions with respect to azimuthal position. The right upper figure (Fig. 5b) shows measured and calculated flap angle variation. The lower figures (Fig.5c) show force and moment variations versus incidence. The movement of both airfoil and flap is in phase: with increasing incidence from start of the period the flap is deflecting downwards (negative β, see Fig. 2).

Comparisons of the two different experimental data sets show the expected differences as can be seen in the C_L versus azimuth curves in Fig. 5a: The extreme values of the lift are measured slightly lower with the balances compared to the results integrated from the Kulites.The latter data are closer to the two dimensional limit and compare therefore better with the numerical data.

The calculated data show higher maxima in lift which must again be attributed to the applied wind tunnel correction procedure: In the present case the nominal mean incidence in the tunnel was 9.1°. After correction this mean value was reduced to 5.7°. However the amplitude was not corrected at all due to the missing of a suitable correction procedure for the dynamic incidence variation as discussed before.

The moment distribution in Fig.5a shows very good correspondence between experiment ("cp") and calculation.

Fig.5: Airfoil in Motion (1/Ref), Flap in Motion (2/Ref), Airfoil and Flap in Phase

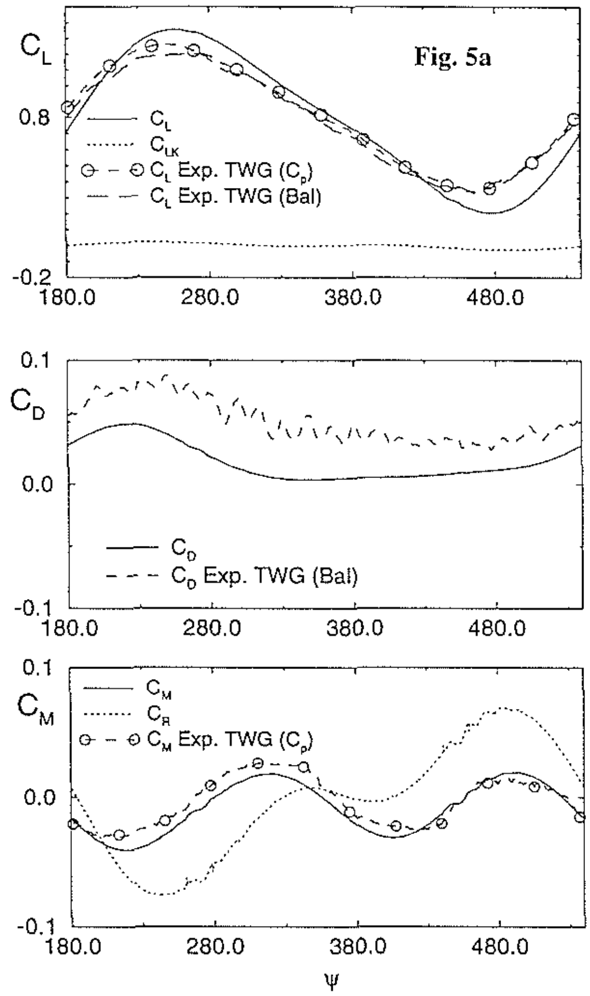

RACT: Airfoil with Moving Flap

$\alpha=5.7^{\circ}+5.2^{\circ}\sin(\omega*T)$

M=0.33

Re=2.03*10[6]

ω*=0.117

β in Phase (2/Ref)

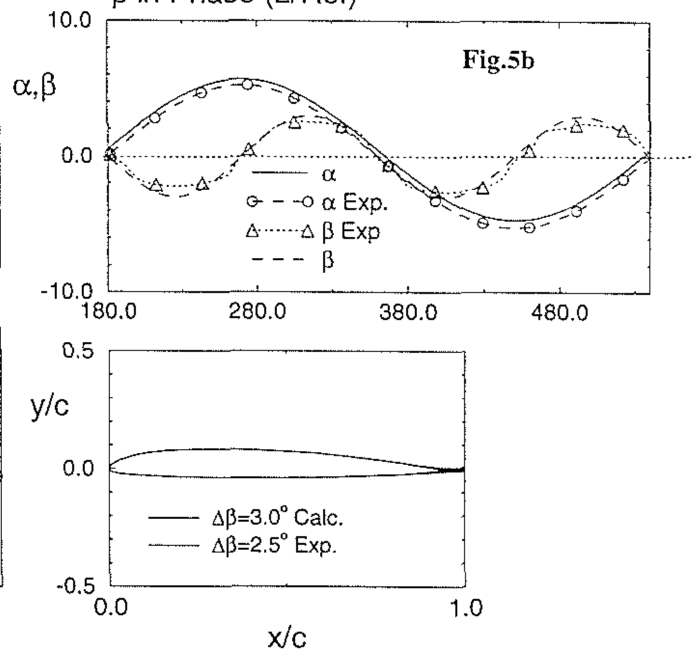

Fig.5c (down): C_L,C_D,C_M Versus Incidence

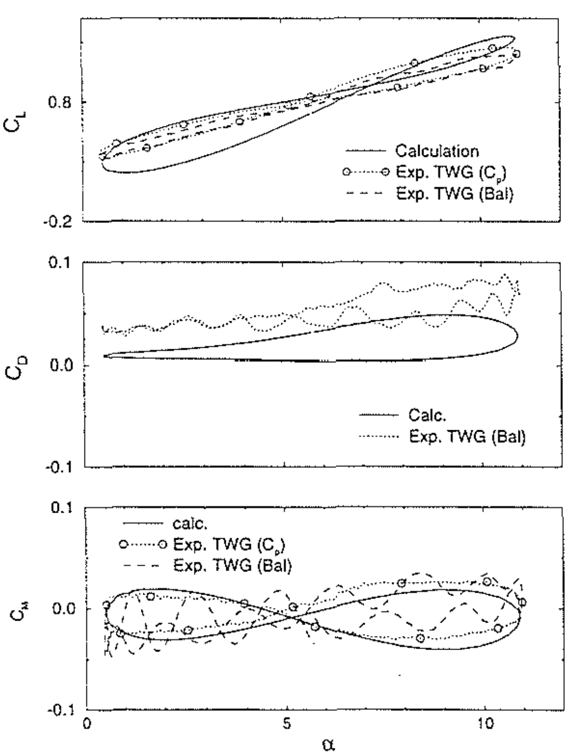

It is obvious that the lift versus azimuth behaves like the 1/ref motion of the airfoil whereas the moment curve is mainly affected by the oscillating flap and therefore shows a 2/ref variation. The moment graph in Fig.5a includes also the calculated flap moment C_R (referred to the flap hinge position). The C_R-distribution indicates that indeed the larger contribution of the overall moment is created at the flap.

The drag coefficient in Fig.5a shows identical unsteady behaviors for both calculation and measurement but the results from the balances are shifted to higher values which again must be attributed to the known steady offset of the piecoelectric balances which has not completely been compensated.

Similar good correspondences between calculation and measurement can be observed in Fig.5c displaying the hysteresis curves of forces and moment versus incidence.

The C_m-loops in Fig.5c include the experimental data measured from the balances. These data show considerable oscillations similar to the C_d-loop. The C_M-loop obtained from the c_p-data again compares very well with calculations.

Fig.6: Airfoil in Motion (1/Ref), Flap in Motion (4/Ref), Airfoil and Flap in Phase

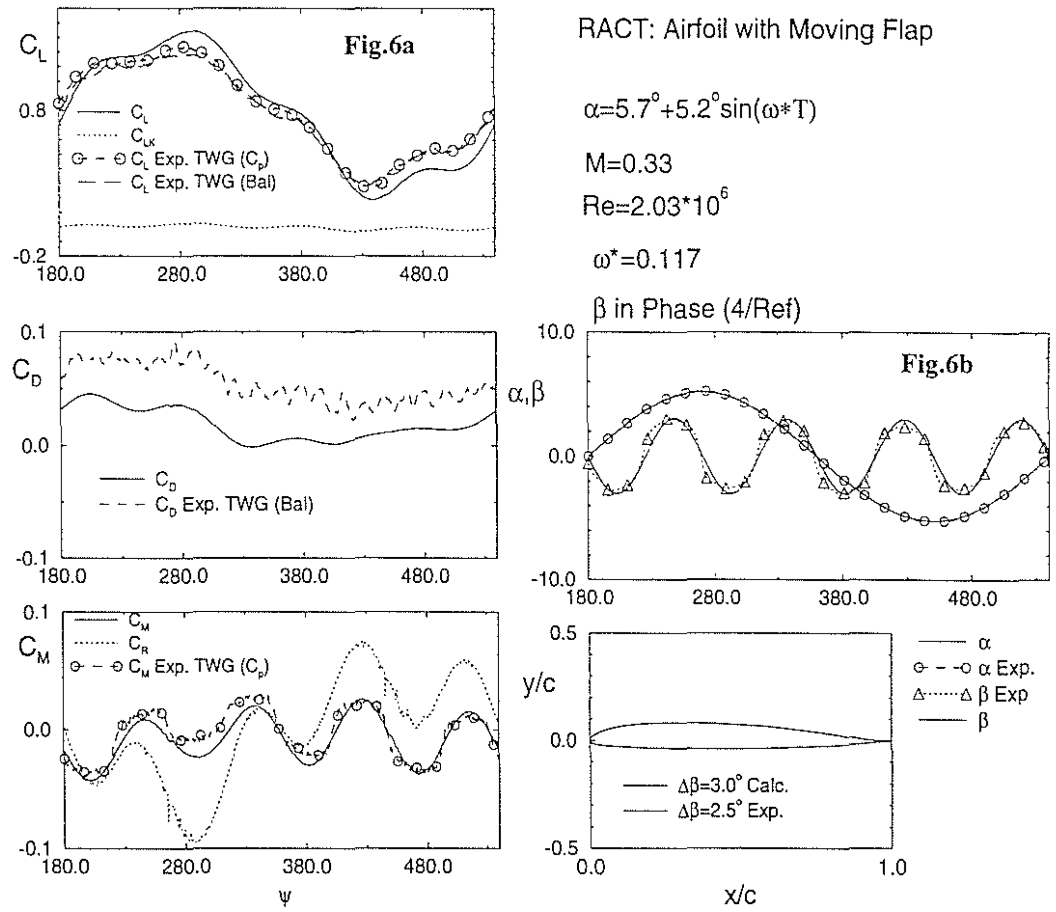

Fig.6c (down) C_L,C_D,C_M Versus Incidence

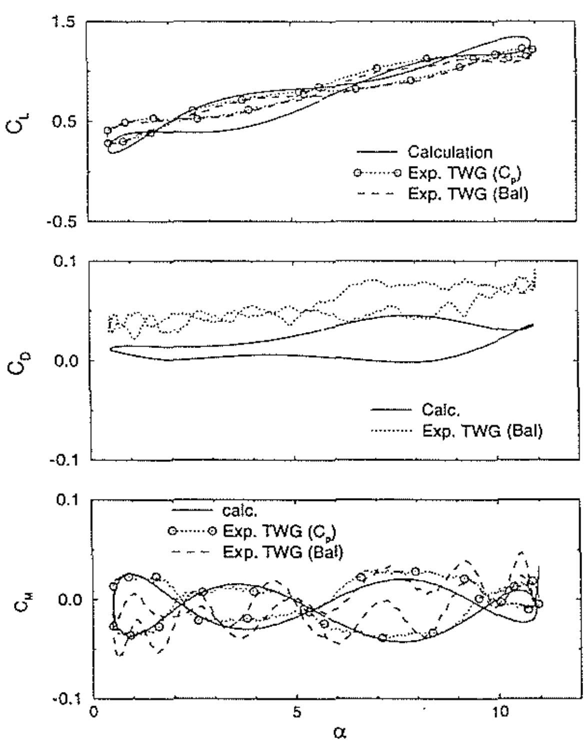

Corresponding results compared to Fig.5 are included in **Fig.6a-c**: Now the flap is oscillating with a frequency of 4/ref i.e. 28Hz in the experimental case. Airfoil and flap are again assumed to move in phase. The lift curve in Fig.6a shows again a 1/ref variation however a 4/ref modulation of this time dependency can clearly be detected. The corresponding moment curve shows the 4/ref time dependency alone. The correspondence between calculation and experiment is very good. The measured drag curve shows again the typical offset as has been discussed before. Similar to the 2/ref case discussed in Fig.5a a small difference in flap amplitude ($\Delta\beta$=2.5^{o} in the experiment compared to $\Delta\beta$=3.0^{o} in the calculation, Fig.6b) may be the source of some small deviations.

The C_m hysteresis loop as indicated in Fig.6c does now show a double-eight structure compared to a single eight in Fig.5c. Also the hysteresis loops of the forces and moment are in good correspondence with the experimental data.

Fig.7: Airfoil in Motion (1/Ref), Flap in Motion (2/Ref), Airfoil and Flap in Phase

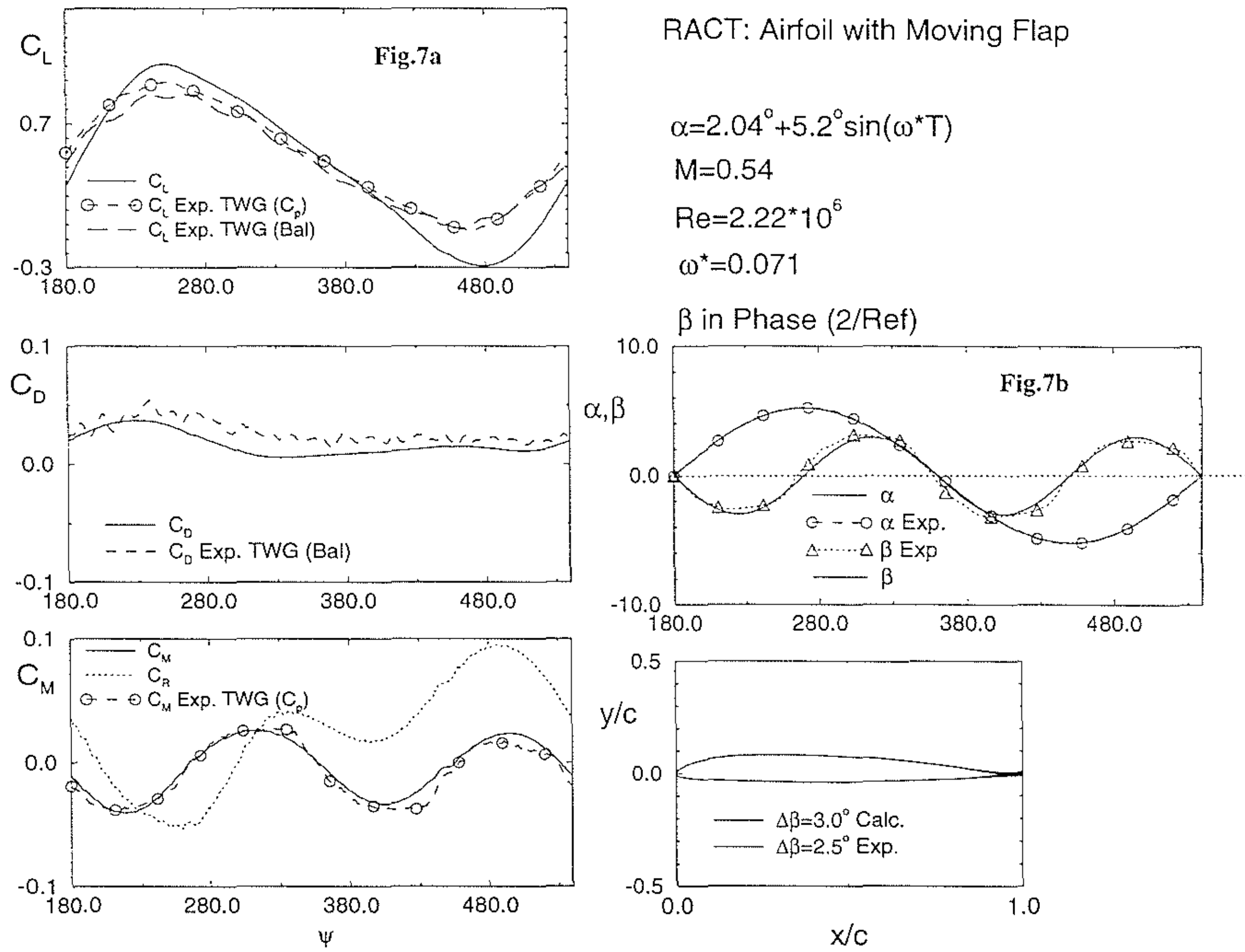

Fig.7c: Pressure- and Skinfriction Distributions

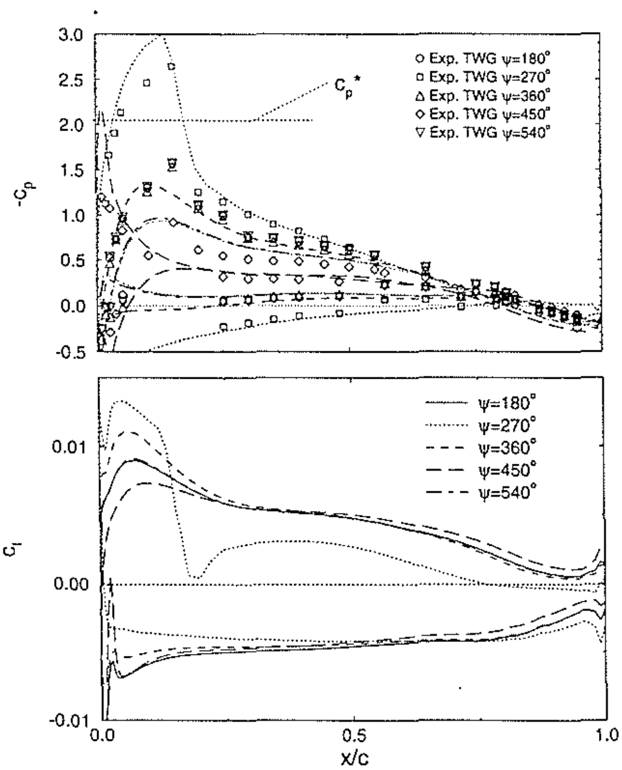

4.3 Machnumber M=0.54.

Figs.7a-c show a 2/ref case again with airfoil and flap motion in phase (see Fig.5.b) at the medium Mach number M=0.54. The nominal mean incidence in the windtunnel was α=4.02°. This value has been corrected to α=2.04° for the 2d- calculations. Again the amplitude for both airfoil and flap motion has not been changed from their wind tunnel values.

The tendencies for force and moment variations with respect to azimuth are similar as discussed in Figs.5 for the low Mach number case. However as can be detected from Fig.7c the pressure distributions clearly show the development of a shock wave over a part of the oscillatory cycle. The shock strength reaches its maximum at about ψ=270° (Fig.7c,upper). At this instant of time the airfoil incidence and the flap deflection have their maximum values with the maximum lift production (see Fig.7a,7b). The corresponding skin friction distribution shows a strong reduction close to zero behind the shock wave (nearly shock induced separation). Along the flap surface the flow is definitely separated for this instant of time (see c_f - distribution at ψ=270°, Fig.7c lower).

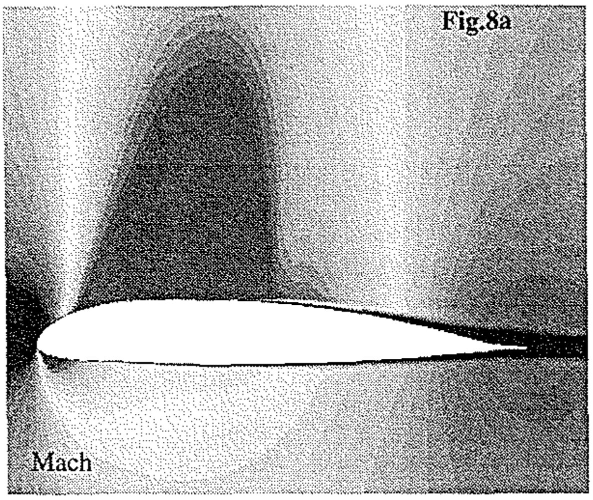

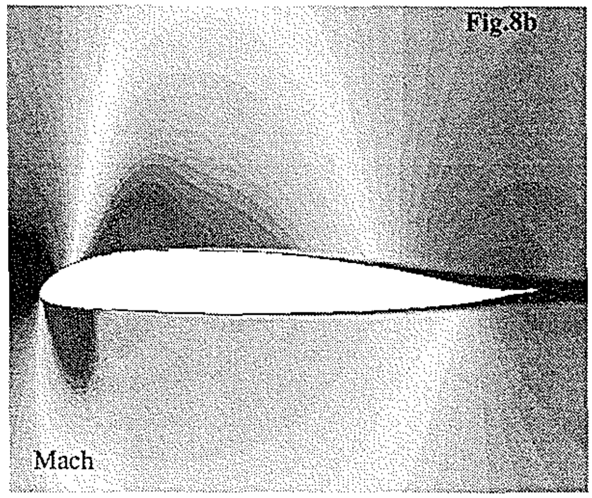

4.4 Machnumber M=0.74.

Increasing compressibility effects are expected at the highest Mach number investigated, i.e. at M=0.74 referring to the advancing rotor blade. In addition the question of wether the piecoelectric actuators would do their job to oscillate the flap with the requested amplitudes and frequencies at this high Mach number could be answered positively.

As a typical example the case of the fixed airfoil with oscillating flap (1/ref, 7Hz) has been selected. Figs.8a and 8b display Mach number contours for the airfoil at a fixed incidence of α=-1.18°, corrected from the nominal wind tunnel value of α=-0.85° (Equation (1)) Fig.8a shows Mach number contours at β=-3° and Fig.8b the corresponding result at β=+3°. A surprisingly strong effect of the moving flap on the Mach number distribution can be detected from these field data: With the flap in its most downward position (left figure) a very strong shock wave is terminating a large supersonic region extending over almost 40% of the front part of the airfoil. With the flap in its most

Fig.8: Airfoil Fixed, Flap in Motion (1/Ref)

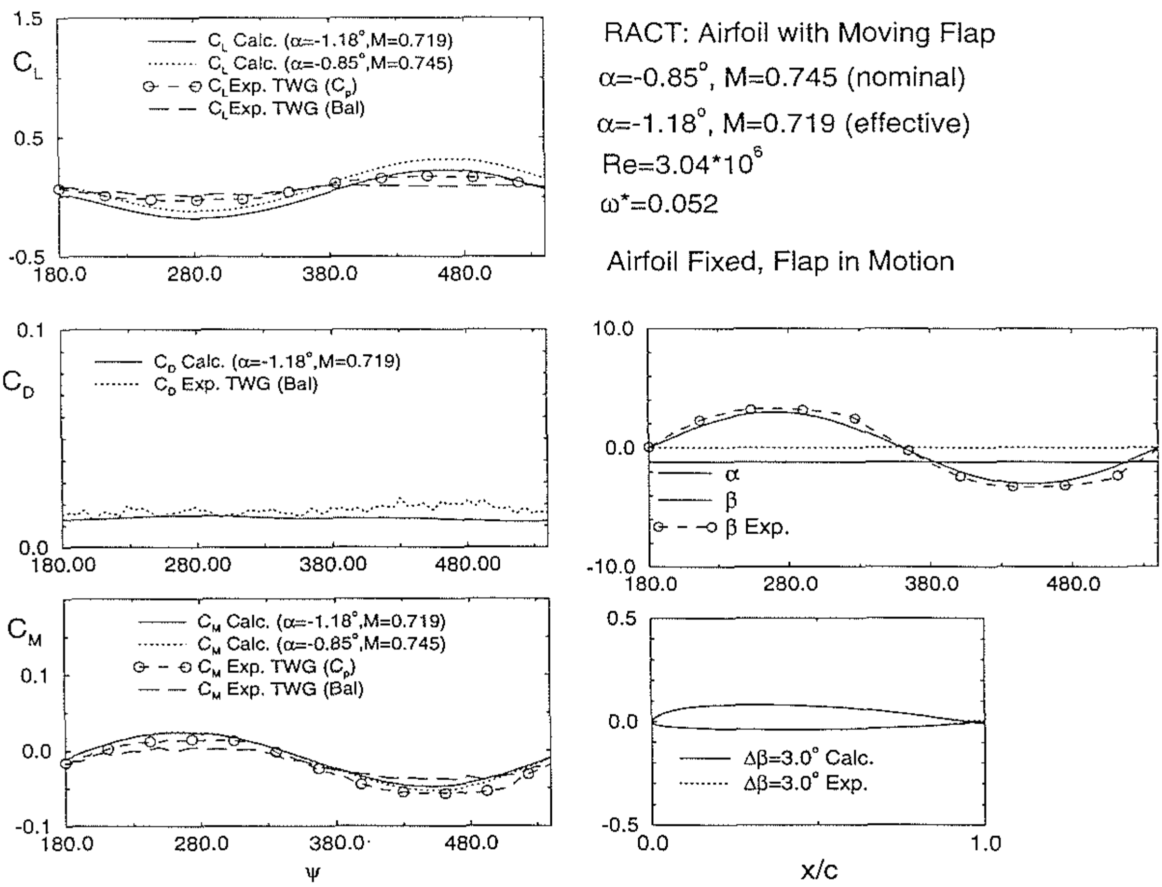

Fig.8c(left): C_L,C_D,C_M Versus Azimuth

Fig.8d(right): Airfoil and Flap Deflection

Fig.8e: Pressure and Skinfriction at Nominal α,M

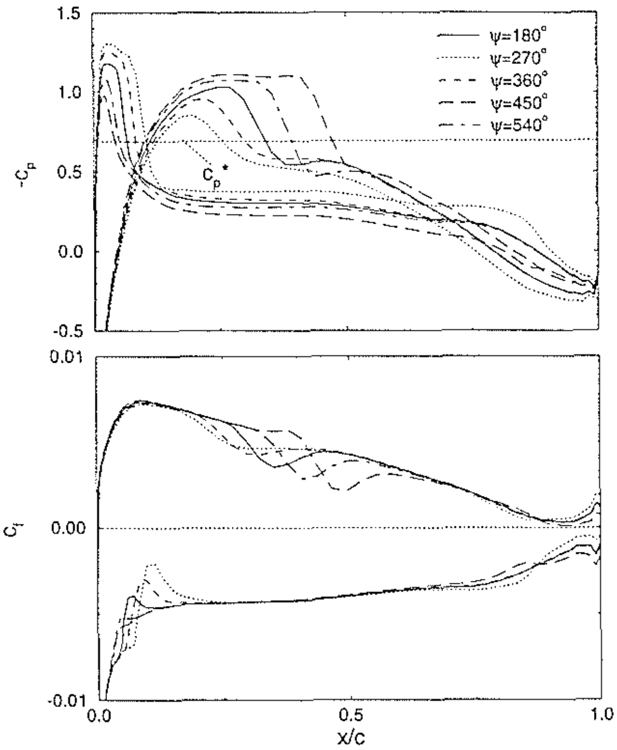

Fig.8f: Pressure and Skinfriction at Effective α,M

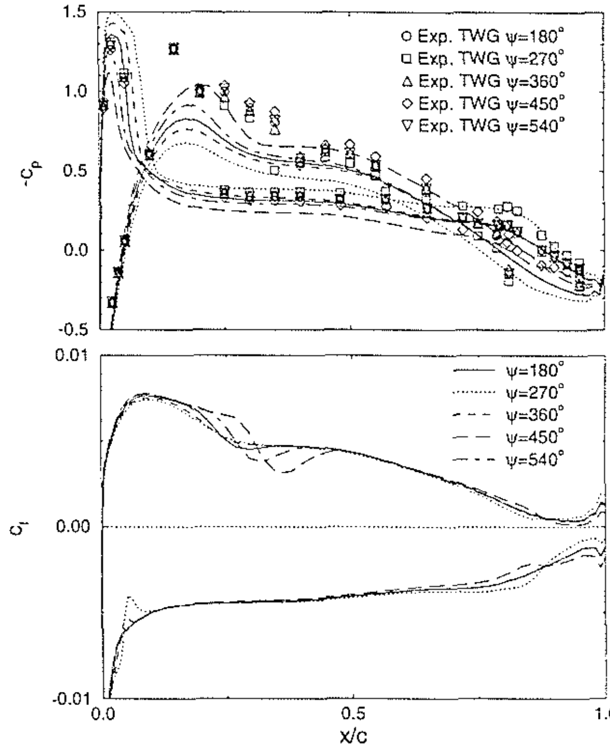

upward position (Fig.8b) the upper surface shock wave has almost disappeared but a small supersonic region also terminated by a shock is developing on the airfoil lower surface close to the leading edge.

Fig.8c shows the corresponding lift-, drag- and pitching moment distributions for this flow case. Again a good correspondence between calculation and experiment can be detected. However in this case the lift curve shows a smaller amplitude in the data compared to the calculation.

The reason for this compared to the previous results unusual large discrepancy has to be investigated more in detail.

Fig.8e shows first pressure and skin friction coefficients for a selected number of time steps of the oscillatory cycle at the nominal Mach number M=0.745. As has been mentioned already before the pressure distributions show the development of a shock wave on the airfoil upper surface which reaches its maximum strength and its most downstream position at maximum lift and correspondingly for the maximum downward flap deflection. With upward moving flap the shock is moving upstream and weakens.

Reaching the most upward flap deflection a shock is developing on the airfoil lower surface adjacent to the leading edge.

However comparing calculated and measured pressures for the present high Machnumber a larger discrepancy is observed: A strong shock wave as has been predicted over part of the oscillatory cycle can not be found in the experimental data.

The previous discussions have shown that at higher

Fig.8g: Pressures at Flap Aerea

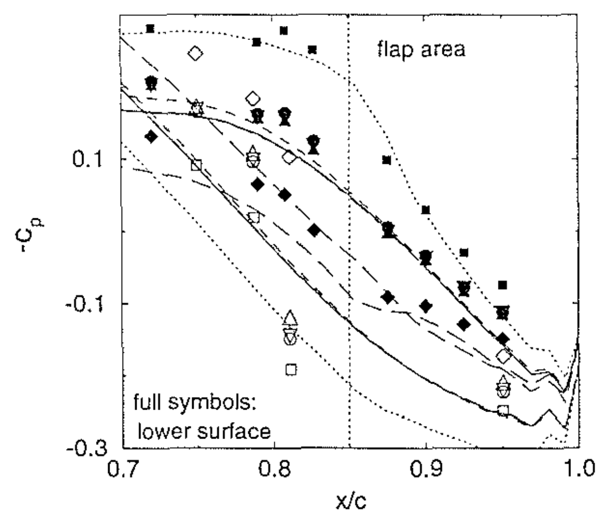

incidences a windtunnel wall correction is necessary to obtain comparable free flight conditions for both calculation and measurement.

It is well known that the perforated walls used in the present experiment make in addition to the incidence correction a Mach number correction necessary. Using the procedure in [11] the correction of the present nominal Mach number M=0.745 leads to the **effective** Machnumber M=0.719 (Equation (2)).

Fig.8f includes numerical data for the reduced Mach number compared to experiment.

Compared to Fig.8e a strong shockwave is now missing. The correspondence between calculation and ex-

periment is considerably improved. The details in the flap area (Fig.8g, symbols are compatible with Fig.8f) show this improvement as well.
In future wind tunnel tests the Mach number correction has to be taken into account in advance to reach the necessary effective Mach number.
Due to the lower effective Mach number in the experiment the maximum lift (at the maximum downward flap deflection (ψ=450°, see fig.8d) is considerably reduced.
Very good correspondence however is achieved for both drag and moment distributions respectively (Fig.8c).

4.5 Animation of Unsteady Field Data

In addition to the present paper a video movie has been developed utilizing the "comadi"-software [13] of the DLR Institute of Fluid Mechanics. The movie shows time dependent periodic flow field data during the motion of the airfoil and/or trailing edge flap.

5. Conclusion.

Within the joint project RACT (Rotor Active Control Technology) between Eurocopter Deutschland (ECD), Deutsches Zentrum für Luft- und Raumfahrt (DLR) and Daimler-Benz Research Institute (DB) a two dimensional wind tunnel model (blade section) for the transonic wind tunnel facility of DLR-Göttingen (TWG) has been built and tested. The model was equipped with a set of four piecoelectric actuators developed by DB and placed completely inside the blade section. The actuators were driving a sealed trailing edge flap of 15% chord length and 0.5m span (half the model span). The model was built and equipped with pressure sensors (Kulites) by the DLR Institute of Flight Mechanics in Braunschweig and suspended in the dynamic testrig of the DLR Institute of Aeroelastic in Göttingen. In addition to the experimental efforts corresponding numerical investigations have been carried out in the DLR Institute of Fluid Mechanics to:
1) Calculate airloads on airfoil and flap for actuator and model design.
2) Recalculate measured steady as well as unsteady flow data in the complete Mach number regime.
3) Investigate the details of the complicated unsteady flows to gain insight into the flow physics involved and to get guide lines for code improvements.
In addition to the numerical efforts the DLR Institute of Fluid Mechanics has carried out some selected tests utilizing the Particle Image Velocimetry (PIV) in particular in the high incidence regime. The PIV measurements were the first of their kind done in the TWG environment.
Model and equipment, actuators, windtunnel test rig and hydraulic model driving system worked perfectly together during the comprehensive wind tunnel test campaign. The main reason for this success was the perfect cooperation between the various test teams of industries and different research institutes of DLR.
In particular the actuator system was able to create amplitudes and frequencies to drive the flap as wanted and did a perfect job during the whole two weeks campaign showing the effectiveness of the actuator system.
As has been outlined in the present paper the correspondence between calculated and measured flow data is very good in all parameter cases investigated so far.
Some major differences had to be attributed to wind tunnel wall influences of the perforated side walls of the test section used for the present test campaign. It has been outlined that a suitable correction procedure known from literature leads to good correspondence between calculation and experiment. In high Mach number flow the nominal Mach number has to be corrected as well and gives a lower effective Mach number which in the present study does not show the compressibility effects predicted by the code. However doing the calculation with the reduced Mach number the correspondence again is good.
In future tests it is recommended to use the available adaptive test section of the TWG to adapt at least both mean incidence and Mach number to free flight conditions. However a correction of the unsteady motion of either flap or airfoil is not straightforward and needs further intensive investigations.
For the future a continuation of the successfull work is envisaged:
The proposal of DLR to dynamically deform the leading edge of a rotor blade to favorably influence the dynamic stall characteristics of the blade has been accepted by industry and corresponding efforts are already underway to realize this idea with a similar actuator technology as has been utilized in the present RACT test.

6. References.

[1] W.Geissler,H.Sobieczky, "Dynamic Stall Control by Variable Airfoil Camber", AGARD 75th Fluid Dynamic Panel Meeting and Symposium on Aerodynamics and Aeroacoustics of Rotorcraft. Oct.10-14,1994,Berlin,Germany.

[2] M.V.Fulton, R.A.Ormiston, "Small-Scale Rotor Experiments with On-blade Elevations to Reduce Blade Vibratory Loads in Forward Flight", American Helicopter Society 54th Annual Forum, Washington,DC,May 20-22,1998.

[3] J.D.Baeder,B.W.Sim, "Blade-Vortex Interaction Noise Reduction by Active Trailing-Edge Flaps", American Helicopter Society 54th Annual Forum, Washington,DC,May 20-22,1998.

[4] D.Schimke,ECD, P.Jänker,DB, A.Blaas,ZFL, R.Kube,DLR, Ch.Kessler,TU-Braunschweig, "Individual Blade Control by Servo-Flap and Blade Root Control", A Collaborative Research and Development Programme. 23th European Rotorcraft Forum, 16-18 Sept., Dresden,Germany.

[5] D.Schimke,ECD,P.Jänker,DB, V.Wendt,B.Junker,DLR, "Windtunnel Evaluation of a Full Scale Piezoelectric Flap Control Unit", 24thEuropean Rotorcraft Forum, Marseille,France,15-17 September,1998.

[6] M.Raffel,T.Dewhirst, "Advanced Flow Velocity Field Metrology and their Application to Helicopter Aerodynamics", 24thEuropean Rotorcraft Forum, Marseille,France,15-17 September,1998.

[7] H.Sobieczky, "Geometry Generation for Transonic Design". Recent Advances in Numerical Methods in Fluids, Vol.4,Ed.W.G.Habashi,Swansea; Pineridge Press, pp.163-182 (1985).

[8] W.Geissler," Instationäres Navier-Stokes Verfahren für beschleunigt bewegte Profile mit Ablösung",DLR-FB 92-03(1992).

[9] W.Geissler,M.S.Chandrasekhara, M.F.Platzer,L.W.Carr,"The Effect of Transition Modeling on the Prediction of Compressible Deep Dynamic Stall", 7th Asian Congress of Fluid Mechanics, Dec. 8-12,1997,Madras,India.

[10] P.R.Spalart,S.R.Allmaras,"A One Equation Turbulence Model for Aerodynamic Flows", 30th Aerospace Sciences Meeting &Exhibit, Jan. 6-9,1992,Reno,NV.

[11] Pindzola, M., LO, C.F., "Boundary Interference at Subsonic Speeds in Wind Tunnels with Ventilated Walls", AEDC-TR-69-47, May 1969.

[12] Garner, H.C., Rogers, E.W.E., Acum, W.E.A., Maskell, E.C., "Subsonic Wind Tunnel Wall Corrections", AGARDograph 109 (Chapter 6.10), Oct. 1966.

[13] H.Vollmers, "The Recovering of Flow Pictures from Large Numerical Data Bases". Lecture Series on 'Comp. Graphics and Flow Visualization in CFD'.VKI,Belgium,Sept. 16-20,1991.